LASER & PHOTONICS REVIEWS

www.lpr-journal.org

Quantum Magnetometer with Dual-Coupling Optomechanics

*Gui-Lei Zhu, Jing Liu, Ying Wu, and Xin-You Lü**

An experimentally feasible magnetometer based on a dual-coupling optomechanical system is proposed, where the radiation-pressure coupling transduces the magnetic signal to the optical phase, and the quadratic optomechanical interaction induces a periodic squeezing effect. The latter not only amplifies the signal to be measured, but also accelerates the signal transducing rate characterized by an experimentally observable phase accumulation efficiency. In the vicinity of opto-mechanical decoupled time, the ultimate bound to the estimability of magnetic signal is proportional to $\exp(-6r)$, and then the optimized accuracy of estimation can be enhanced nearly three orders with a controllable squeezing parameter $r < 1$. Moreover, this proposal is robust against the mechanical thermal noise, and the sensitivity of a specific measurement can reach to the order of $10^{-17}\mathrm{T}(\sqrt{\mathrm{Hz}})^{-1}$ in the presence of dissipations and without ground state cooling of mechanical oscillator. The proposal fundamentally broadens the fields of quantum metrology and cavity optomechanics, with the potential application for on-chip magnetic detection with high precision.

1. Introduction

Ultrasensitive magnetic detection has contributed immensely to a wide range of scientific areas from fundamental physics to advanced technologies, such as geological exploration, aerospace,[1] biomedical imaging, and diagnostics.[2–4] Over the past few decades, various magnetometers have been developed, including the superconducting quantum interference devices (SQUID) based on superconducting effects,[5–7] spin-exchange relaxation-free atomic magnetometers,[8–11] NV center magnetometers,[12,13] and Hall-effect sensors.[14] Normally, they require the elaborated operating conditions, such as the associated denoising technology and/or the complex signal read-out schemes,[15] which reduce their capability of on-chip integration.

G.-L. Zhu, J. Liu, Y. Wu, X.-Y. Lü
School of Physics
Huazhong University of Science and Technology
Wuhan 430074, China
E-mail: xinyoulu@hust.edu.cn

J. Liu
MOE Key Laboratory of Fundamental Physical Quantities Measurement and PGMF
Huazhong University of Science and Technology
Wuhan 430074, China

The ORCID identification number(s) for the author(s) of this article can be found under https://doi.org/10.1002/lpor.202100636

DOI: 10.1002/lpor.202100636

Cavity optomechanical system (OMS)[16–19] offers an alternative platform for the precision measurements of mass,[20–22] weak forces,[23–27] and magnetic fields.[28–33] Particularly, optomechanical magnetometer with high precision has excellent quality of on-chip integration.[34] Recently, the YIG sphere-based optomechanical magnetometer has been experimentally demonstrated in ref. [35], which has attained extremely low sensitivity values. In such magnetometers, the existence of Joule and Villari effects of magnetostrictive transducer,[36] allows one to directly extract magnetic information by reading out the optical frequency shift (or transmission spectrum). Moreover, quantum metrology[37–40] points out that the quantum squeezing or entanglement[41–48] could improve the accuracy of parameter estimation in physical systems from the shot-noise limit to the Heisenberg limit, that is, the optimal precision scales from $1/\sqrt{N}$ to $1/N$ with N being the number of resources employed in the measurements. This has stimulated enormous interests in exploiting quantum resources in the atoms (or spins)[49–52] and optical systems[53–56] for high-precision physical quantity measurements. By applying quantum metrology to the detection of a static magnetic field, here we propose a quantum magnetometer based on a dual-coupling OMS, which has a periodic decoupling behavior between the optical and mechanical modes. The OMS supports two optical modes coupled simultaneously to the same mechanical mode, with radiation-pressure and quadratic optomechanical interactions, respectively.[57–60] The radiation-pressure coupling acts as a signal transducer, encoding the magnetic signal received by the mechanical oscillator into the optical phase. The quadratic optomechanical interaction amplifies both the signal to be measured and the signal transducing rate via inducing a periodic squeezing effect on the mechanical oscillator, whose maximum squeezing strength is determined by a controllable squeezing parameter r. By performing a homodyne detection on the optical phase within a wide time window around the first decoupled time τ_1, the magnetic signal could be estimated with high precision.

To qualitatively characterize the precision of magnetometer, we define a displaced phase accumulation efficiency (PAE) that is experimentally observable via state tomography technique. By presenting the *exponentially* increased quantum Fisher information (QFI), that is, $\mathcal{F}_{\mathrm{q}}(\tau_1) \propto \mathrm{e}^{12r}$, we quantitatively demonstrate

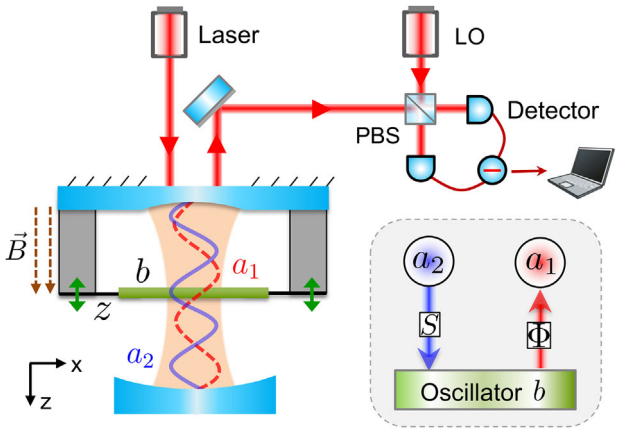

Figure 1. Schematic illustration of quantum magnetometer based on a dual-coupling OMS with "membrane-in-the-middle" configuration. The middle SiN membrane (green), acting as the mechanical mode b, is welded to the ends of magnetostrictive Terfenol-D rods (gray).[61] On application of a static magnetic field, the Terfenol-D rods expands, which displaces the equilibrium position of the mechanical mode, and then the magnetic signal is encoded into the phase Φ of optical mode a_1 via radiation-pressure coupling. Besides, cavity mode a_2 offers the periodic squeezing for mode b via the quadratic optomechanical interaction (see the shaded area). The optical phase is detected by the balanced homodyne detection scheme with a local oscillator (LO) pulse.

that the fundamental bound of measurement precision can be dramatically reduced even with a small squeezing parameter r. The periodic opto-mechanical decoupling makes the classical Fisher information (CFI) robust against the mechanical environment at the decoupled time, which in turn allows the sensitivity of a specific measurement to saturate the fundamental bound and reach to the order of $10^{-17}\mathrm{T}(\sqrt{\mathrm{Hz}})^{-1}$ in the presence of system dissipations. Moreover, the sensitivity to the order of $10^{-15}\mathrm{T}(\sqrt{\mathrm{Hz}})^{-1}$ is predicted even in the case of the thermal phonon number $\bar{n}_{\mathrm{th}} \approx 10^3$. Our work establishes a connection between quantum metrology and dual-coupling optomechanics, which is suitable for detecting various fields that linearly interact with the mechanical oscillator.

2. System and Periodic Mechanical Squeezing

We consider a dual-coupling optomechanical system depicted in **Figure 1** with Hamiltonian

$$H = \hbar\omega_1 a_1^\dagger a_1 + \hbar\omega_2 a_2^\dagger a_2 + \hbar\omega_{\mathrm{m}} b^\dagger b - \hbar\lambda_1 a_1^\dagger a_1 (b^\dagger + b) - \hbar\lambda_2 a_2^\dagger a_2 (b^\dagger + b)^2 + B_z c_{\mathrm{act}} z \quad (1)$$

where a_j $(j = 1, 2)$ and b are the annihilation operators of the cavity mode with frequency ω_j and the mechanical mode with frequency ω_{m}, respectively. The mechanical membrane is placed at a node (antinode) of cavity mode a_1 (a_2), and then the fourth (fifth) term in Equation (1) describes the radiation-pressure (quadratic optomechanical) interaction between modes a_1 (a_2) and b with strength λ_1 (λ_2). In the presence of a static magnetic field B_z (along z direction), the field-sensitive Terfenol-D expands, which leads to the change of the equilibrium position of the mechanical oscillator, thus generating an effective magnetic potential on the Hamiltonian, that is, the last term of Equation (1).[62] The mechanical motion modulates the optical cavity field via the nonlinear radiation-pressure coupling. Meanwhile, the phase shift of the mechanical motions encoded with magnetic signal is transferred to the optical field. By reading out the phase shift of optical field via homodyne detection, we can extract the original magnetic information. Here $z = \sqrt{\hbar/(2m\omega_{\mathrm{m}})}(b^\dagger + b)$ is the position operator of the mechanical oscillator with mass m, and $c_{\mathrm{act}} = m\omega_{\mathrm{m}}^2 L\alpha_{\mathrm{mag}}/E$ is the magnetic actuation constant characterizing how well the magnetic field is converted into a force applied on the oscillator. The symbol L denotes the length of Terfenol-D rods, α_{mag} is magnetostrictive coefficient, and E is the Young's modulus.[62]

By considering the ancillary mode a_2 in the coherent state $|\xi\rangle$, the number operator $a_2^\dagger a_2$ can be approximately replaced by an algebraic number $\mathcal{N}_2 = |\xi|^2$ in the case of $\mathcal{N}_2 \gg 1$.[62] Assuming the modes a_1 and b are initially in the coherent state $|\Psi(0)\rangle = |\alpha\rangle \otimes |\beta\rangle$ with $\beta = \beta_{\mathrm{Re}} + i\beta_{\mathrm{Im}}$, the instantaneous state of system is given by[62]

$$|\Psi(t)\rangle = e^{-|\alpha|^2/2} \sum_{n=0}^{\infty} \frac{\alpha^n}{\sqrt{n!}} \exp\left[i\eta^2(\omega_{\mathrm{s}} t - \sin\omega_{\mathrm{s}} t)\right] \times \exp\{i\eta[\beta_{\mathrm{Re}} \sin\omega_{\mathrm{s}} t e^{-r} - \beta_{\mathrm{Im}}(\cos\omega_{\mathrm{s}} t - 1)e^{r}]\}|n\rangle|\varphi_{\mathrm{s}}(t)\rangle \quad (2)$$

where $\eta = \lambda_{\mathrm{s}} n/\omega_{\mathrm{s}} - f_{\mathrm{s}}/\omega_{\mathrm{s}}$ with $\lambda_{\mathrm{s}} = \lambda_1 e^r$, $\omega_{\mathrm{s}} = \omega_{\mathrm{m}} e^{-2r}$, $f_{\mathrm{s}} = fe^r = B_z c_{\mathrm{act}}\sqrt{1/(2m\hbar\omega_{\mathrm{m}})}e^r$, $r = -(1/4)\ln(1 - 4\lambda_2\mathcal{N}_2/\omega_{\mathrm{m}})$, and a rotating frame with $\exp(-i\omega_1 a_1^\dagger a_1/\omega_{\mathrm{s}})$ was adopted. The mechanical state reads $|\varphi_{\mathrm{s}}(t)\rangle = S^\dagger(r)S(r')|\varphi_n(t)\rangle$ with the defined squeezing operator $S(r) = \exp[r(b^2 - b^{\dagger 2})/2]$ and the squeezing parameter $r' = re^{-2i\omega_{\mathrm{s}} t}$. Here $|\varphi_n(t)\rangle = |e^{-i\omega_{\mathrm{s}} t}\beta + \eta\bar{\mu}\rangle$ is a displaced coherent state with $\bar{\mu} = (1 - e^{-i\omega_{\mathrm{s}} t})(\cosh r - e^{-i\omega_{\mathrm{s}} t}\sinh r)$. The expression of $|\varphi_{\mathrm{s}}(t)\rangle$ clearly shows that the mechanical mode is dynamically squeezed with the period $T = \pi/\omega_{\mathrm{s}}$, whose squeezing degree of quadrature $X = 1/\sqrt{2}(b + b^\dagger)$ is defined by $S(t) = 10\log_{10}(\delta X^2(t)/\delta X^2_{\mathrm{min}})\mathrm{dB}$. The maximum squeezing degree $S_{\mathrm{max}} = 10\log_{10}(e^{4r})\mathrm{dB}$ occurs at $T/2$ with the state $S^\dagger(2r)|\beta\rangle$.[62] This periodic squeezing effect on the mechanical oscillator is induced by the quadratic optomechanical coupling, and can be qualitatively presented in the case of $\alpha = \eta = 0$ (see **Figure 2**a).

3. Periodic-Squeezing-Enhanced Phase Accumulation Efficiency

As shown in Equation (2), the magnetic signal is transduced into the optical phase during the evolution of system via the radiation–pressure interaction. Interestingly, at time $\tau_{\mathrm{m}} = 2m\pi/\omega_{\mathrm{s}}$ $(m = 1, 2, \ldots)$, Equation (2) can be reduced to[62]

$$|\Psi(\tau_{\mathrm{m}})\rangle = e^{-|\alpha|^2/2} \sum_{n=0}^{\infty} \frac{\alpha^n}{\sqrt{n!}} e^{i\Phi_n(\tau_{\mathrm{m}})}|n\rangle|\beta\rangle \quad (3)$$

which demonstrates that the optical and mechanical modes are periodically decoupled, meanwhile the magnetic signal to be measured is periodically encoded into the accumulated optical

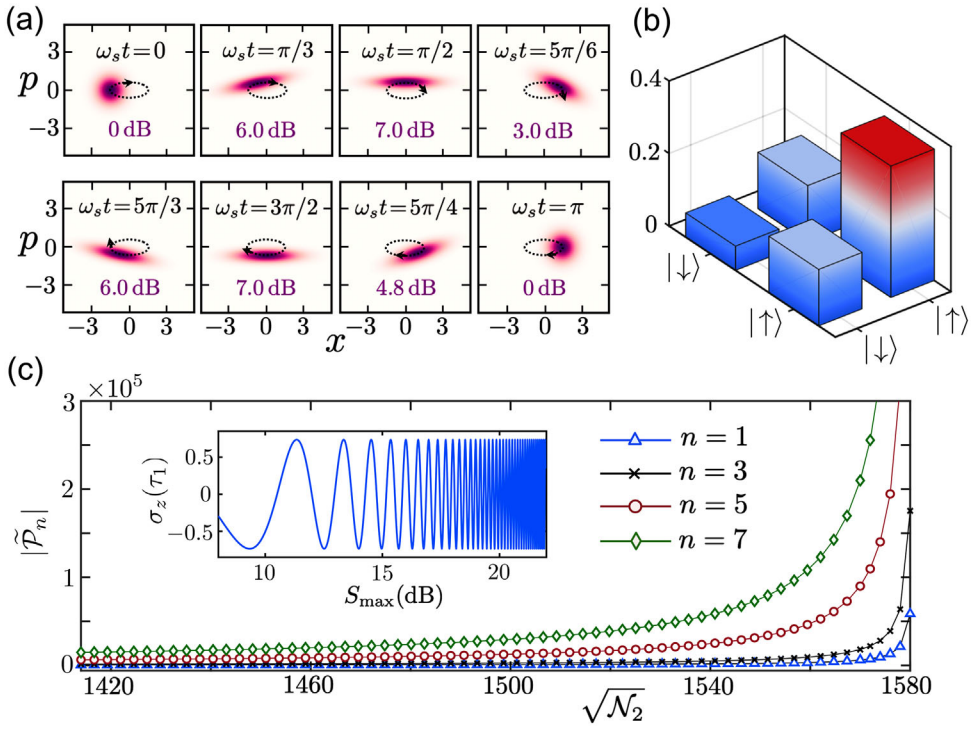

Figure 2. a) Wigner functions of the mechanical mode within $2T$ given by a_1 in vacuum state $|0\rangle$, $\omega_m = 1$ and $\sqrt{\mathcal{N}_2} = 1414$. The instantaneous squeezing degrees are marked. b) Tomography of the state $|\Psi(\tau_1)\rangle$ projected on the subsapce $\{|\downarrow\rangle, |\uparrow\rangle\}$ with $l = 3$ and $\sqrt{\mathcal{N}_2} = 1500$. The dependence of $\sigma_z(\tau_1)$ on the maximum squeezing degree $S_{\max}$ for $l = 1$ and $f = \omega_m$ is shown in the insert of (c). The main panel of (c) shows the absolute value of displaced PAE $|\widetilde{\mathcal{P}}_n|$ as a function of $\sqrt{\mathcal{N}_2}$ for several values of n. The parameters are $\omega_m = 2\pi \times 134$kHz, $f = 0.01\omega_m$, $\alpha = 1$, $\lambda_1 = 0.01\omega_m$, and $\lambda_2 = 10^{-7}\omega_m$.

phase $\Phi_n(\tau_m) = 2m\pi(\lambda_s n/\omega_s - f_s/\omega_s)^2$ for a Fock state $|n\rangle$. Here the opto-mechanical decoupled period is double of the period of dynamical squeezing, that is, $\tau_1 = 2\pi/\omega_s = 2T$, and hence the mechanical squeezing also disappears at the decoupled time τ_m.

The above unique property allows us to estimate the magnetic field B_z by performing a homodyne detection (see Figure 1) on the optical mode a_1 at the first decoupled time τ_1. To qualitatively describe the detection precision, here we define a displaced PAE

$$\widetilde{\mathcal{P}}_n = \frac{\Phi_n(\tau_1) - \Phi_0(\tau_1)}{\tau_1} = \frac{\lambda_1 n}{\omega_m}(\lambda_1 n - 2f)e^{4r} \tag{4}$$

Obviously, the larger $\widetilde{\mathcal{P}}_n$, that is, the faster phase accumulation rate on the optical Fock state $|n\rangle$, the higher measurement accuracy of magnetometer should be obtained. As shown in Figure 2c, the $\widetilde{\mathcal{P}}_n$ is exponentially enhanced by increasing the coherent amplitude $\sqrt{\mathcal{N}_2}$ of the ancillary mode a_2. This enhancement originally comes from the periodic squeezing of mechanical mode during one opto-mechanical decoupled period (see Figure 2a). The system Hamiltonian in the squeezed frame shown in Equation S17, Supporting Information[62] clearly demonstrates that the mechanical squeezing effect not only accelerates the signal transducing rate from phonon to photon (i.e., the radiation–pressure interaction $\lambda_s a_1^\dagger a_1(b + b^\dagger)$),[63,64] but also amplifies the magnetic signal to be measured (i.e., the magnetic potential $f_s(b^\dagger + b)$).

More importantly, this well-defined PAE is experimentally observable via state tomography in the proper basis vectors. Specifically, expanding the system state $|\Psi(\tau_1)\rangle$ in the subspace $\{|\downarrow\rangle, |\uparrow\rangle\}$ with basis vectors $|\downarrow\rangle := (1/\sqrt{2})(|0\rangle - |l\rangle)$ and $|\uparrow\rangle := (1/\sqrt{2})(|0\rangle + |l\rangle)$ $(l = 1, 2, \ldots)$, we obtain four elements of density matrix,[62] as shown in Figure 2b. The difference between two diagonal elements is denoted by $\sigma_z(\tau_1) = \rho_{\uparrow\uparrow}(\tau_1) - \rho_{\downarrow\downarrow}(\tau_1) = 2e^{-|\alpha|^2}(\alpha^l/\sqrt{l!})\cos(\Delta\Phi_l(\tau_1))$, where $\Delta\Phi_l(\tau_1) = \Phi_l(\tau_1) - \Phi_0(\tau_1)$. Then one can easily obtain the values of phase difference $\Delta\Phi_l(\tau_1)$ by directly measuring $\rho_{\downarrow\downarrow}(\tau_1)$ and $\rho_{\uparrow\uparrow}(\tau_1)$, which ultimately leads to $\widetilde{\mathcal{P}}_l = \Delta\Phi_l(\tau_1)/\tau_1$ being experimentally observable. Moreover, the oscillation with increasing frequency of $\sigma_z(\tau_1)$, shown in the insert of Figure 2c, is another evidence for the enhanced $\widetilde{\mathcal{P}}_n$ along with increasing the mechanical squeezing.

4. Quantum and Classical Fisher Information

From a quantitative point of view, the fundamental bound to the sensitivity and the measurement-specific sensitivity of the proposed magnetometer are respectively decided by the QFI $\mathcal{F}_q$ and CFI $\mathcal{F}_c$ based on the Cramér–Rao inequality $\Delta B_z \geq 1/\sqrt{M\mathcal{F}_j}$ $(j = q, c)$, where ΔB_z is the standard deviation with respect to an unbiased estimator $(B_z)_{est}$, and M is the number of repetition of the experiments.[65]

Considering system state $|\Psi(t)\rangle$, the QFI with respect to the parameter B_z reads

$$\mathcal{F}_q(t) = 4(\langle\partial_{B_z}\Psi(t)|\partial_{B_z}\Psi(t)\rangle - \left|\langle\Psi(t)|\partial_{B_z}\Psi(t)\rangle\right|^2) \tag{5}$$

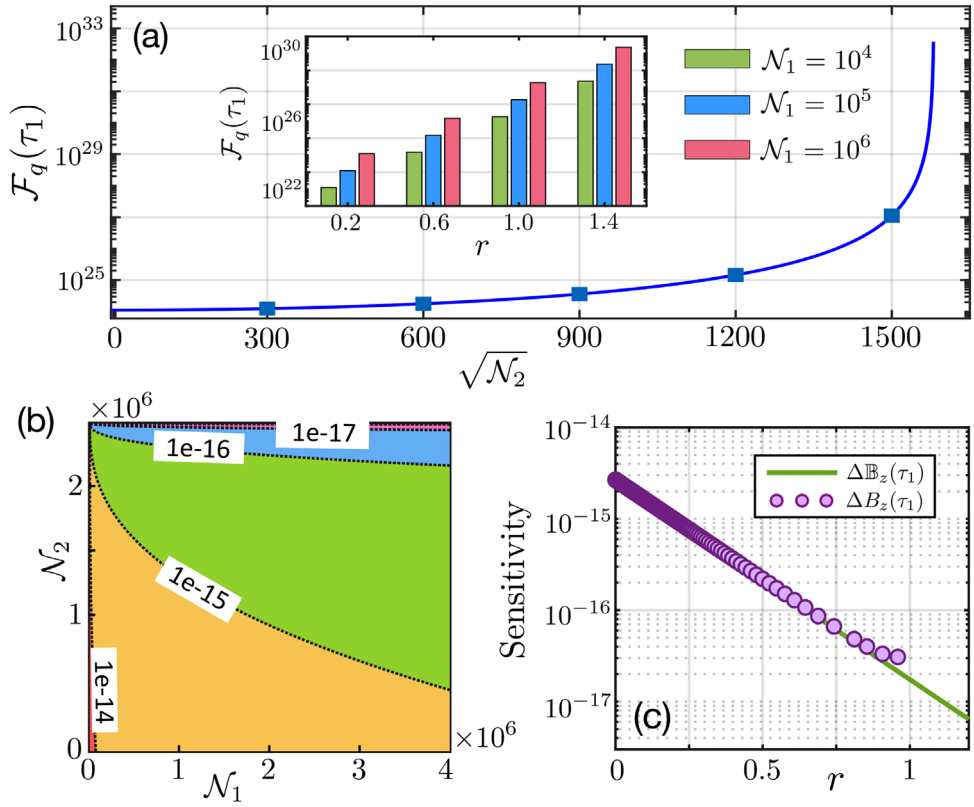

Figure 3. a) The QFI $\mathcal{F}_q(\tau_1)$ versus $\sqrt{\mathcal{N}_2}$ (main) and r (inset). b) Contourf plot of the optimal sensitivity $\Delta\mathbb{B}_z(\tau_1)$ in units of $\mathrm{T}(\sqrt{\mathrm{Hz}})^{-1}$ as functions of $\mathcal{N}_1$ and $\mathcal{N}_2$. c) $\Delta\mathbb{B}_z(\tau_1)$ (solid curve) and the specific sensitivity $\Delta B_z(\tau_1)$ in the presence of dissipations (circles) versus r for $\mathcal{N}_1 = 10^6$. Here we have chosen $m = 4\times10^{-8}$g, $L = 630\mu$m, $\alpha_{\mathrm{mag}} = 5\times10^8\mathrm{NT}^{-1}\mathrm{m}^{-1}$, $E = 30$GPa, $\kappa/\omega_{\mathrm{m}} = 0.01$, $\gamma/\omega_{\mathrm{m}} = 0.001$, $\bar{n}_{\mathrm{th}} = 10$ and other parameters are same as Figure 2.

where $\partial_{B_z} = \partial/\partial_{B_z}$.[66–70] At the first decoupled time τ_1, the QFI reduces to[62]

$$\mathcal{F}_q(\tau_1) = \frac{32\pi^2 m\lambda_1^2 L^2\alpha_{\mathrm{mag}}^2}{\hbar\omega_{\mathrm{m}}E^2}\mathcal{N}_1 e^{12r} = \frac{32\pi^2 m\lambda_1^2 L^2\alpha_{\mathrm{mag}}^2}{\hbar\omega_{\mathrm{m}}E^2}\frac{\mathcal{N}_1}{[1-(4\lambda_2/\omega_{\mathrm{m}})\mathcal{N}_2]^3} \tag{6}$$

where $\mathcal{N}_1 = |\alpha|^2$ is the mean photon number of cavity mode a_1. It can be seen that the QFI is exponentially enhanced with power of $12r$, and hence increasing a small value of r by changing $\mathcal{N}_2$ can give rise to a large enhancement of the QFI. **Figure 3**a shows an enhancement with seven orders of magnitude for the QFI, corresponding to a dramatic reduction of the optimal sensitivity $\Delta\mathbb{B}_z(\tau_1) = 1/\sqrt{M\mathcal{F}_q(\tau_1)}$. As shown in Figure 3b, the optimal sensitivity $\Delta\mathbb{B}_z(\tau_1)$ can reach to the order of $10^{-15}-10^{-17}(\mathrm{T}(\sqrt{\mathrm{Hz}})^{-1}$ for a wide parameter region in terms of the mean photon numbers $\mathcal{N}_1$ and $\mathcal{N}_2$. Equation (6) also indicates that the resources $\mathcal{N}_1$ and $\mathcal{N}_2$ exert different influences on the ultimate lower bound of sensitivity.[62] We note that the QFI at τ_1 does not depend on the actual value of B_z.

Next, let us calculate the CFI related to a specific measurement on the quadrature $X_\theta = (a_1 e^{-i\theta} + a_1^\dagger e^{i\theta})/\sqrt{2}$, where θ is the phase of local oscillator. At the first decoupled time τ_1, the CFI is given by[62]

$$\mathcal{F}_c(\tau_1) = \frac{32\pi^2 m\lambda_1^2 L^2\alpha_{\mathrm{mag}}^2}{\hbar\omega_{\mathrm{m}}E^2}e^{12r}(\alpha_{\mathrm{Re}}\sin\theta - \alpha_{\mathrm{Im}}\cos\theta)^2 \tag{7}$$

Evidently, it consists precisely with the QFI shown in Equation (6) when $\theta = \pi/2$ ($\theta = 0$) and α is a real (imaginary) number, which means that the momentum (position) measurement can saturate the optimal sensitivity in the absence of system dissipation.

In the practical situation, the dissipation caused by the system-bath coupling should be taken into account. Then the dynamics of system is dominated by the master equation

$$\dot{\rho} = -\frac{i}{\hbar}[H,\rho] + \kappa\mathcal{D}[a_1]\rho + \gamma(\bar{n}_{\mathrm{th}}+1)\mathcal{D}[b]\rho + \gamma\bar{n}_{\mathrm{th}}\mathcal{D}[b^\dagger]\rho \tag{8}$$

where $\kappa(\gamma)$ is the cavity (mechanical) decay rate, $\bar{n}_{\mathrm{th}}$ is the thermal phonon number of the mechanical mode, and $\mathcal{D}[o]\rho = o\rho o^\dagger - (o^\dagger o\rho + \rho o^\dagger o)/2$. Here we have considered the cavity mode a_2 being in the coherent state $|\xi\rangle$ for Hamiltonian H. Performing a momentum homodyne measurement (i.e., $\theta = \pi/2$) on cavity a_1, in Figures 3c and 4, we numerically demonstrate the influence of system dissipation on the sensitivity limit, that is, $\Delta B_z(\tau_1) = 1/\sqrt{M\mathcal{F}_c(\tau_1)}$, of magnetometer.[71]

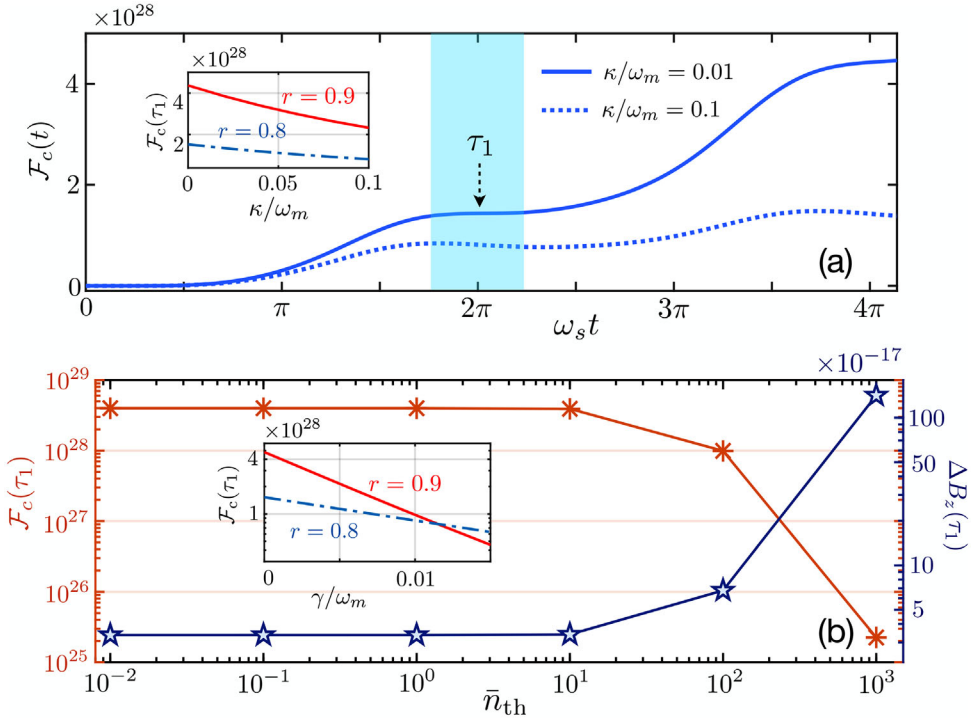

Figure 4. a) Time evolution of $\mathcal{F}_c(t)$ for different values of κ/ω_m in the presence of mechanical dissipation $\gamma/\omega_m = 0.01$, $\bar{n}_{\rm th} = 10$ and considering $r = 0.8$. The shaded area indicates the time-window of detection with nearly flat $\mathcal{F}_c(t)$ in the vicinity of the first decoupled time τ_1. b) CFI $\mathcal{F}_c(\tau_1)$ (left y-axis) and specific sensitivity $\Delta B_z(\tau_1)$ in units of $\mathrm{T}(\sqrt{\mathrm{Hz}})^{-1}$ (right y-axis) versus mechanical thermal phonon number $\bar{n}_{\rm th}$ for $\kappa/\omega_m = 0.01$ and $\gamma/\omega_m = 0.001$. The insets show the influence of κ and γ on $\mathcal{F}_c(\tau_1)$ for different values of squeezing parameter r.

With the practical experimental parameters, Figure 3c shows that the specific sensitivity $\Delta B_z(\tau_1)$ obtained in the presence of system decay and noise, still can fit well with the optimal one $\Delta \mathbb{B}_z(\tau_1)$ from the QFI without system dissipation. This consistency is only broken weakly when one increases the squeezing parameter r to a large value. This can be explained as follows. On the one hand, system dissipation has little effect on the CFI $\mathcal{F}_c(\tau_1)$ in the case of weak squeezing parameter r (see the inserts of Figure 4). More importantly, the periodic optomechanical decoupling makes the CFI robust against the mechanical thermal noise. As shown in Figure 4b, a high sensitivity reaching to the order of $10^{-15}\mathrm{T}(\sqrt{\mathrm{Hz}})^{-1}$ is allowed even when $\bar{n}_{\rm th} = 10^3$. This means that the mechanical ground state cooling is not necessary for obtaining high-precision magnetometer in our proposal. On the other hand, the strong mechanical squeezing amplifies the effect of mechanical dissipation on CFI via effectively heating the environment (see the insert of Figure 4b and Figure S5, Supporting Information), which leads to the weak disagreement between the measurement-specific sensitivity limit and the fundamental bound of sensitivity in the case of large values of r.

5. Discussion of Experimental Feasibility

Regarding experimental implementations, while we have considered here a Febry–Pérot cavity with the membrane-in-the-middle configuration, our versatile proposal is not limited to this particular architecture. Based on the excellent controllability of the SQUID,[72,73] the transmission-line (TL) resonator coupled to a SQUID-terminated TL resonator is a promising platform to realize dual-coupling optomechanical system.[74,75] Recently, the dual-coupling optomechanics was also demonstrated in photonic crystal cavities[76,77] and whispering gallery microcavities.[78] Based on recent optomechanical experiments,[57,58,79] here the system parameters can be chosen as $m = 4 \times 10^{-8}$ g, $\omega_{\rm m} = 2\pi \times 134$ kHz, $\lambda_1 = 8.4$ kHz, $\lambda_2 = 0.08$ Hz, $\kappa = 8.4$ kHz, $\gamma = 840$ Hz, and $\mathcal{N}_1 = 10^6$. Then, with a cycle time on tens of μs, our work theoretically predicts that the sensitivity in the range of $10^{-15} - 10^{-17}\mathrm{T}(\sqrt{\mathrm{Hz}})^{-1}$ can be realized with the achievable squeezing parameter $r \in [0, 0.9]$. Note that most of the above results are obtained in the case of performing the homodyne measurement at the first decoupled time τ_1. Fortunately, our proposal is robust against the detection time, that is, the CFI in the vicinity of τ_1 is nearly flat as shown in Figure 4a. In other words, our proposal exhibits a wide time-window to perform measurement with sensitivity reaching to the order of $10^{-17}\mathrm{T}(\sqrt{\mathrm{Hz}})^{-1}$.

Moreover, the experimental implementation of our proposal relies on the thin membrane held by Terfenol-D rods, which gives an effective magnetic potential on the Hamiltonian. The conversion efficiency from the applied magnetic field to an effective force on the mechanical oscillator, is determined by the magnetic actuation constant $c_{\rm act}$. The precise experimental determination of the magnetic actuation constant is of key importance for measuring afterwards accurate values of the magnetic field. This magnetic constant depends heavily on the specific geomet-

rical configuration of the rods with respect to the membrane. To optimize the magnetostrictive effect, the applied magnetic field needs to be paralleled to the magnetostricitive direction of the Terfenol-D rods. In addition, here we considered the Terfenol-D rods of the length $\approx 10^{-5}$ m, thus it is approximatively valid to consider the magnetostrictive material to be in the whole homogeneous magnetic field, which also allows the system to have a large actuation constant.

Despite here we focus on detecting a static magnetic field, our proposal, in principle, can also be applied to probe the alternating magnetic fields. The corresponding frequency response characteristics are discussed in Section S7, Supporting Information.[62] Referring to the parameters used in optomechanical experiments,[34,57] we numerically simulate the displacement noise power spectrum and the corresponding force sensitivity at different probe powers (see Figure S6, Supporting Information). We find that the thermal-noise-limited frequency range covers 0∼380 kHz with the central resonant frequency 250 kHz in the case of the probe power at 20nW. Therefore, similar as a general optomechanical system,[34] here the dual-coupling magnetometer also has a broad bandwidth, when it is used as a resonant sensor.

6. Conclusions

We have presented a protocol to measure the weak magnetic field using dual-coupling optomechanics. The sensitivity could be enhanced to the order of $10^{-15} - 10^{-17}\mathrm{T}(\sqrt{\mathrm{Hz}})^{-1}$ by adjusting the photon numbers of two cavity modes. This enhancement originally comes from the periodic mechanical squeezing, which greatly amplifies both the signal to be measured and the transducing rate of signal. We stress out that this periodic squeezing effect is self-sustained, which avoids the complicated process of preparing squeezed states. Our proposal, with wide time-window of detection, is robust against the mechanical thermal noise, and hence the ground state cooling of mechanical mode is not necessary. This work might inspire the studies of high-precision measurements of various physical quantities based on dual-coupling optomechanical systems.

Supporting Information

Supporting Information is available from the Wiley Online Library or from the author.

Acknowledgements

The authors thank Bei-Bei Li for fruitful discussions and valuable comments. This work was supported by the National Key Research and Development Program of China grant 2021YFA1400700, the National Science Foundation of China (grant nos. 11822502, 11974125, 11875029, 12175075, and 11805073).

Conflict of Interest

The authors declare no conflict of interest.

Data Availability Statement

The data that support the findings of this study are available in the Supporting Information of this article.

Keywords

cavity optomechanics, magnetometer, periodic squeezing, precision measurements

Received: November 7, 2021
Revised: April 6, 2022
Published online: July 1, 2022

[1] J. S. Bennett, B. E. Vyhnalek, H. Greenall, E. M. Bridge, F. Gotardo, S. Forstner, G. I. Harris, F. A. Miranda, W. P. Bowen, *Sensors* **2021**, *21*, 5568.
[2] M. Hämäläinen, R. Hari, R. J. Ilmoniemi, J. Knuutila, O. V. Lounasmaa, *Rev. Mod. Phys.* **1993**, *65*, 413.
[3] H. Lee, T.-H. Shin, J. Cheon, R. Weissleder, *Chem. Rev.* **2015**, *115*, 10690.
[4] D. Murzin, D. J. Mapps, K. Levada, V. Belyaev, A. Omelyanchik, L. Panina, V. Rodionova, *Sensors* **2020**, *20*, 1569.
[5] R. C. Jaklevic, J. Lambe, A. H. Silver, J. E. Mercereau, *Phys. Rev. Lett.* **1964**, *12*, 159.
[6] S. N. Erné, H.-D. Hahlbohm, H. Lübbig, *J. Appl. Phys.* **1976**, *47*, 5440.
[7] R. Kleiner, D. Koelle, F. Ludwig, J. Clarke, *Proc. IEEE* **2004**, *92*, 1534.
[8] J. C. Allred, R. N. Lyman, T. W. Kornack, M. V. Romalis, *Phys. Rev. Lett.* **2002**, *89*, 130801.
[9] I. K. Kominis, T. W. Kornack, J. C. Allred, M. V. Romalis, *Nature* **2003**, *422*, 596.
[10] I. M. Savukov, S. J. Seltzer, M. V. Romalis, K. L. Sauer, *Phys. Rev. Lett.* **2005**, *95*, 063004.
[11] H. Xia, A. Ben-Amar Baranga, D. Hoffman, M. V. Romalis, *Appl. Phys. Lett.* **2006**, *89*, 211104.
[12] J. M. Taylor, P. Cappellaro, L. Childress, L. Jiang, D. Budker, P. R. Hemmer, A. Yacoby, R. Walsworth, M. D. Lukin, *Nat. Phys.* **2008**, *4*, 810.
[13] J. R. Maze, P. L. Stanwix, J. S. Hodges, S. Hong, J. M. Taylor, P. Cappellaro, L. Jiang, M. V. G. Dutt, E. Togan, A. S. Zibrov, A. Yacoby, R. L. Walsworth, M. D. Lukin, *Nature* **2008**, *455*, 644.
[14] S. J. Bending, *Adv. Phys.* **1999**, *48*, 449.
[15] D. Robbes, *Sens. Actu. A: Phys.* **2006**, *129*, 86.
[16] M. Aspelmeyer, T. J. Kippenberg, F. Marquardt, *Rev. Mod. Phys.* **2014**, *86*, 1391.
[17] T. J. Kippenberg, K. J. Vahala, *Science* **2008**, *321*, 1172.
[18] M. Aspelmeyer, P. Meystre, K. Schwab, *Phys. Today* **2012**, *65*, 29.
[19] P. Meystre, *Ann. Phys.* **2013**, *525*, 215.
[20] J.-J. Li, K.-D. Zhu, *Appl. Phys. Lett.* **2012**, *101*, 141905.
[21] Q. Lin, B. He, M. Xiao, *Phys. Rev. A* **2017**, *96*, 043812.
[22] S.-W. Bin, X.-Y. Lü, T.-S. Yin, G.-L. Zhu, Q. Bin, Y. Wu, *Opt. Lett.* **2019**, *44*, 630.
[23] A. A. Clerk, M. H. Devoret, S. M. Girvin, F. Marquardt, R. J. Schoelkopf, *Rev. Mod. Phys.* **2010**, *82*, 1155.
[24] M. Tsang, C. M. Caves, *Phys. Rev. Lett.* **2010**, *105*, 123601.
[25] A. Pontin, M. Bonaldi, A. Borrielli, F. S. Cataliotti, F. Marino, G. A. Prodi, E. Serra, F. Marin, *Phys. Rev. A* **2015**, *89*, 023848.
[26] F. Armata, L. Latmiral, A. D. K. Plato, M. S. Kim, *Phys. Rev. A* **2017**, *96*, 043824.
[27] S. Qvarfort, A. Serafini, P. F. Barker, S. Bose, *Nat. Commun.* **2018**, *9*, 3690.

[28] S. Forstner, S. Prams, J. Knittel, E. D. van Ooijen, J. D. Swaim, G. I. Harris, A. Szorkovszky, W. P. Bowen, H. Rubinsztein-Dunlop, *Phys. Rev. Lett.* **2012**, *108*, 120801.
[29] S. Forstner, E. Sheridan, J. Knittel, C. L. Humphreys, G. A. Brawley, H. Rubinsztein-Dunlop, W. P. Bowen, *Adv. Mater.* **2014**, *26*, 6348.
[30] C. Yu, J. Janousek, E. Sheridan, D. L. McAuslan, H. Rubinsztein-Dunlop, P. K. Lam, Y. Zhang, W. P. Bowen, *Phys. Rev. Appl.* **2016**, *5*, 044007.
[31] M. Wu, N. L.-Y. Wu, T. Firdous, F. Fani Sani, J. E. Losby, M. R. Freeman, P. E. Barclay, *Nat. Nanotechnol.* **2017**, *12*, 127.
[32] J. Zhu, G. Zhao, I. Savukov, L. Yang, *Sci. Rep.* **2017**, *7*, 8896.
[33] B.-B. Li, J. Bílek, U. B. Hoff, L. S. Madsen, S. Forstner, V. Prakash, C. Schäfermeier, T. Gehring, W. P. Bowen, U. L. Andersen, *Optica* **2018**, *5*, 850.
[34] B.-B. Li, L. Ou, Y. Lei, Y.-C. Liu, *Nanophotonics* **2021**, *10*, 2799.
[35] M. F. Colombano, G. Arregui, F. Bonell, N. E. Capuj, E. Chavez-Angel, A. Pitanti, S. O. Valenzuela, C. M. Sotomayor-Torres, D. Navarro-Urrios, M. V. Costache, *Phys. Rev. Lett.* **2020**, *125*, 147201.
[36] A. Olabi, A. Grunwald, *Mater. Des.* **2008**, *29*, 469.
[37] V. Giovannetti, S. Lloyd, L. Maccone, *Science* **2004**, *306*, 1330.
[38] V. Giovannetti, S. Lloyd, L. Maccone, *Phys. Rev. Lett.* **2006**, *96*, 010401.
[39] V. Giovannetti, S. Lloyd, L. Maccone, *Nat. Photon.* **2011**, *5*, 222.
[40] J. P. Dowling, K. P. Seshadreesan, *J. Lightwave Technol.* **2015**, *33*, 2359.
[41] C. M. Caves, *Phys. Rev. D* **1981**, *23*, 1693.
[42] J. Ma, X. Wang, C. Sun, F. Nori, *Phys. Rep.* **2011**, *509*, 89.
[43] T. Baumgratz, A. Datta, *Phys. Rev. Lett.* **2016**, *116*, 030801.
[44] C. L. Degen, F. Reinhard, P. Cappellaro, *Rev. Mod. Phys.* **2017**, *89*, 035002.
[45] N. J. Engelsen, R. Krishnakumar, O. Hosten, M. A. Kasevich, *Phys. Rev. Lett.* **2017**, *118*, 140401.
[46] T. Nagata, R. Okamoto, J. L. O'Brien, K. Sasaki, S. Takeuchi, *Science* **2007**, *316*, 726.
[47] Y. Israel, S. Rosen, Y. Silberberg, *Phys. Rev. Lett.* **2014**, *112*, 103604.
[48] X.-Y. Luo, Y.-Q. Zou, L.-N. Wu, Q. Liu, M.-F. Han, M. K. Tey, L. You, *Science* **2017**, *355*, 620.
[49] J. A. Jones, S. D. Karlen, J. Fitzsimons, A. Ardavan, S. C. Benjamin, G. A. D. Briggs, J. J. L. Morton, *Science* **2009**, *324*, 1166.
[50] T. Tanaka, P. Knott, Y. Matsuzaki, S. Dooley, H. Yamaguchi, W. J. Munro, S. Saito, *Phys. Rev. Lett.* **2015**, *115*, 170801.
[51] P. Kómár, E. M. Kessler, M. Bishof, L. Jiang, A. S. Sørensen, J. Ye, M. D. Lukin, *Nat. Phys.* **2014**, *10*, 582.
[52] Z. Hou, Z. Zhang, G.-Y. Xiang, C.-F. Li, G.-C. Guo, H. Chen, L. Liu, H. Yuan, *Phys. Rev. Lett.* **2020**, *125*, 020501.
[53] M. J. Holland, K. Burnett, *Phys. Rev. Lett.* **1993**, *71*, 1355.
[54] A. N. Boto, P. Kok, D. S. Abrams, S. L. Braunstein, C. P. Williams, J. P. Dowling, *Phys. Rev. Lett.* **2000**, *85*, 2733.
[55] P. M. Anisimov, G. M. Raterman, A. Chiruvelli, W. N. Plick, S. D. Huver, H. Lee, J. P. Dowling, *Phys. Rev. Lett.* **2010**, *104*, 103602.
[56] J. Joo, W. J. Munro, T. P. Spiller, *Phys. Rev. Lett.* **2011**, *107*, 083601.
[57] J. D. Thompson, B. M. Zwickl, A. M. Jayich, F. Marquardt, S. M. Girvin, J. G. E. Harris, *Nature* **2008**, *452*, 72.
[58] J. C. Sankey, C. Yang, B. M. Zwickl, A. M. Jayich, J. G. E. Harris, *Nat. Phys.* **2010**, *6*, 707.
[59] M. Bhattacharya, H. Uys, P. Meystre, *Phys. Rev. A* **2008**, *77*, 033819.
[60] G.-L. Zhu, X.-Y. Lü, L.-L. Wan, T.-S. Yin, Q. Bin, Y. Wu, *Phys. Rev. A* **2018**, *97*, 033830.
[61] C. Hong, *Mater. Des.* **2013**, *46*, 617.
[62] See more details in Supporting Information.
[63] X.-Y. Lü, Y. Wu, J. R. Johansson, H. Jing, J. Zhang, F. Nori, *Phys. Rev. Lett.* **2015**, *114*, 093602.
[64] M.-A. Lemonde, N. Didier, A. A. Clerk, *Nat. Commun.* **2016**, *7*, 11338.
[65] S. L. Braunstein, C. M. Caves, *Phys. Rev. Lett.* **1994**, *72*, 3439.
[66] M. G. A. Paris, *Int. J. Quantum Inf.* **2009**, *07*, 125.
[67] G. Tóth, I. Apellaniz, *J. Phys. A: Math. Theor.* **2014**, *47*, 424006.
[68] J. Liu, H. Yuan, X.-M. Lu, X. Wang, *J. Phys. A: Math. Theor.* **2019**, *53*, 023001.
[69] X.-M. Lu, X. Wang, *Phys. Rev. Lett.* **2021**, *126*, 120503.
[70] J. Liu, M. Zhang, H. Chen, L. Wang, H. Yuan, *Adv. Quantum Technol.* **2022**, *5*, 2100080.
[71] J. Johansson, P. Nation, F. Nori, *Comput. Phys. Commun.* **2012**, *183*, 1760.
[72] J. Q. You, F. Nori, *Nature* **2011**, *474*, 589.
[73] Z.-L. Xiang, S. Ashhab, J. Q. You, F. Nori, *Rev. Mod. Phys.* **2013**, *85*, 623.
[74] J. R. Johansson, G. Johansson, F. Nori, *Phys. Rev. A* **2014**, *90*, 053833.
[75] E.-j. Kim, J. R. Johansson, F. Nori, *Phys. Rev. A* **2015**, *91*, 033835.
[76] M. Kalaee, T. K. Paraïso, H. Pfeifer, O. Painter, *Opt. Express* **2016**, *24*, 21308.
[77] M. Brunelli, O. Houhou, D. W. Moore, A. Nunnenkamp, M. Paternostro, A. Ferraro, *Phys. Rev. A* **2018**, *98*, 063801.
[78] H.-K. Li, Y.-C. Liu, X. Yi, C.-L. Zou, X.-X. Ren, Y.-F. Xiao, *Phys. Rev. A* **2012**, *85*, 053832.
[79] C. F. Ockeloen-Korppi, E. Damskägg, J.-M. Pirkkalainen, M. Asjad, A. A. Clerk, F. Massel, M. J. Woolley, M. A. Sillanpää, *Nature* **2018**, *556*, 478.